

# Quantum phase transitions of two-species bosons in square lattice

Pochung Chen<sup>1,\*</sup> and Min-Fong Yang<sup>2</sup>

<sup>1</sup>*Department of Physics, National Tsing Hua University, Hsinchu 30013, Taiwan*

<sup>2</sup>*Department of Physics, Tunghai University, Taichung 40704, Taiwan*

(Dated: September 16, 2010)

We investigate various quantum phase transitions of attractive two-species bosons in a square lattice. Using the algorithm based on the tensor product states, the phase boundaries of the pair superfluid states with nonzero pair condensate density *and* vanishing atomic condensate density are determined. Various quantum phase transitions across the phase boundaries are characterized. Our work thus provides guides to the experimental search of the pair superfluid phase in lattice boson systems.

Ultracold atoms in optical lattices provide an unprecedented toolbox for the experimental realization of exotic quantum phases which are not easily accessible in condensed matter systems [1]. Recent experimental demonstration of the superfluid-to-Mott transition for ultracold bosons in an optical lattice [2], for example, has paved the way for studying other strongly correlated phases in various lattice models. Among these systems, Bose-Bose, Fermi-Fermi, and Bose-Fermi mixtures have attracted considerable attention, since a variety of interesting ordered states can be realized in such systems [1]. In particular, it has been suggested that, for the mixture of two bosonic species in a lattice, interspecies repulsion and attraction can give rise to additional incompressible super-counterfluid (SCF) and compressible pair superfluid (PSF) phases, respectively [3–17]. Furthermore, when the intra-species nearest-neighbor repulsion is included, the counterflow supersolid and the pair-supersolid phases may also emerge [17].

The quantum phase of our interest is the PSF phase of two-species hard-core bosons on a square lattice with interspecies attraction  $U_{ab} (< 0)$ , which is described by the Hamiltonian,

$$H = -t \sum_{\langle ij \rangle} (a_i^\dagger a_j + b_i^\dagger b_j + \text{h.c.}) - \mu \sum_{i, \sigma} n_i^\sigma + U_{ab} \sum_i n_i^a n_i^b, \quad (1)$$

where  $\sigma = a, b$  indicates the two species and  $n_i^\sigma$  is the particle densities at site  $i$ . The intra-species tunneling is denoted by  $t > 0$  and  $\mu$  is the chemical potential. The symbol  $\langle ij \rangle$  indicates nearest neighbors. When  $|U_{ab}|/t \gg 1$ , the PSF phase can be stabilized by forming a superfluid of boson pairs of different species [9–17]. This phase is characterized by a nonzero pair condensate density  $n_0^{\text{PSF}} \equiv |\langle ab \rangle|^2 \neq 0$  *and* a vanishing atomic condensate densities  $n_0^\sigma \equiv |\langle \sigma \rangle|^2 = 0$ . By considering two species as two components of spin-1/2 particles, it implies from the symmetry breaking perspective that the “charge”  $U(1)$  symmetry  $a \rightarrow e^{i\theta} a$ ;  $b \rightarrow e^{i\theta} b$  is broken spontaneously in the PSF phase, while the “spin”  $U(1)$

symmetry  $a \rightarrow e^{i\varphi} a$ ;  $b \rightarrow e^{-i\varphi} b$  is not. Here  $\theta$  and  $\varphi$  denote the angles of the corresponding  $U(1)$  rotations. The PSF phase hence can also be identified by a nonzero pair-superfluid density  $\rho_s^{\text{PSF}} \propto \langle (W_a + W_b)^2 \rangle \neq 0$  *and* a zero super-counterfluid density  $\rho_s^{\text{SCF}} \propto \langle (W_a - W_b)^2 \rangle = 0$ , where  $W_\sigma$  are the winding numbers for bosons of species  $\sigma$  [18]. By contrast, the two miscible superfluid (2SF) phase is expected in the opposite limit of  $|U_{ab}|/t \ll 1$ , where both species form superfluids with nonzero atomic condensate density  $n_0^a, n_0^b \neq 0$ . In addition to the distinct properties of the PSF states, intriguing quantum phase transitions out of this phase can occur. Based on the analysis of the mean-field theory, it was proposed that [10], for the cases of spatial dimensions being larger than one, the PSF-2SF transitions can be either second or first order, while the PSF to Mott insulating (MI) phase transitions are always second order.

While the existence of a PSF phase of lattice boson has been pointed out in the literature using various approaches [9–17], direct calculations of microscopic quantum models with large sizes has not yet been reported except for the one-dimensional case [12–14]. This is perhaps due to the difficulty in analyzing these quantum models by applying conventional methods. For example, despite quantum Monte Carlo (QMC) simulation being free from the sign problem for this model, several practical technical issues may still hinder high-precision large-scale QMC calculations. Firstly, multi-worm algorithm needs to be implemented [7, 11, 19], because standard single-worm algorithm may converge quite slowly in the PSF states. Secondly, very low temperatures are necessary to detect the pair superfluid coherence in the PSF phase. This is due to that the effective hopping of *pairs* is about the order of  $t^2/|U_{ab}|$  [3, 4] and is quite small since  $t/|U_{ab}| \ll 1$  in the PSF phase. Finally, systems of large enough sizes should be considered in order to determine phase transitions being of either *weakly* first order or second order. Therefore, accurate quantitative predictions of associated quantum phase transitions in the thermodynamical limit around the PSF phase remain under investigation.

In this paper, various quantum phase transitions of the model in Eq. (1) are investigated. We would set  $|U_{ab}| \equiv 1$  as the energy unit. Due to the particle-hole symmetry in the present hard-core model, the phase diagram is sym-

\*Electronic address: pcchen@phys.nthu.edu.tw

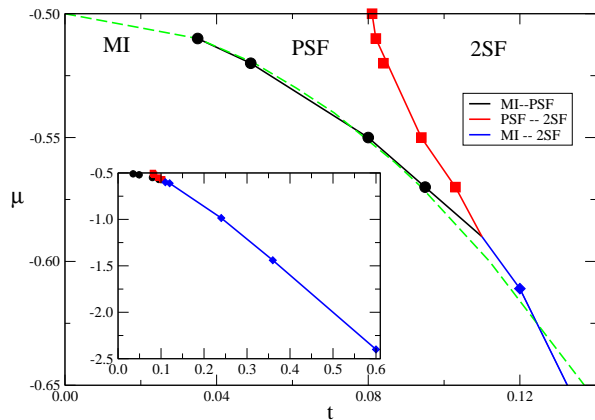


FIG. 1: (Color online) Ground-state phase diagram of attractive two-species hard-core bosons on a square lattice of size  $2^7 \times 2^7$  as described in Eq. (1) with  $|U_{ab}| = 1$ . Solid lines are guide to eyes. The green dashed line gives the analytic estimate of the MI-PSF phase boundary (see text). The inset shows the phase diagram in a larger scale.

metric with respect to the line  $\mu = -1/2$ , at which the average density for each species becomes  $1/2$ . It is therefore sufficient to concentrate on the parameter region of  $\mu \leq -1/2$  where both species are below half filling. Our main purpose is to determine quantitatively the phase boundaries of the PSF phase and to reveal the nature of these quantum phase transitions. Here the combined algorithm [20] of the infinite time-evolving block decimation (iTEBD) method [21] and the tensor renormalization group (TRG) approach [22] is exploited. The success of this method in obtaining accurate physical quantities at zero temperature of systems with large sizes has been demonstrated for several quantum spin systems [20, 23–26]. Since systems of two-species hard-core bosons can be mapped onto anisotropic spin-1/2 bilayer spin models, from our previous experience on the study of the frustrated bilayer spin models [24], the employed approach is expected to give reliable results for the present issues. The resulting phase diagram is shown in Fig. 1. The region of the PSF phase with finite pair condensate but zero atomic condensate is discovered, and the phase boundaries out of the PSF state are determined precisely. The nature of various transitions is found to be in agreement with that proposed in Ref. [10]. Our findings hence provide further theoretical support on searching the PSF phases in the bosonic systems with mutual attraction. However, we stress that the PSF phase is stabilized only within a limited region of the zero-temperature phase diagram in Fig. 1. Therefore, carefully tuning system parameters into the suggested parameter regime is necessary to uncover experimentally this novel phase.

To characterize different phases, several local order parameters are evaluated. Because the hopping parameter and the chemical potential in Eq. (1) are set to be equal for both species, equal densities for the two species ( $n^a = n^b$ ) are expected. In our calculations we do find

that the exchanging symmetry between two species is always unbroken and the expectation values for  $a$  and  $b$  bosons are the same. Consequently, we show only the results of species  $a$  as representatives. When the average density of single species boson  $n = (1/N_s) \sum_i \langle n_i^a \rangle$  becomes an integer (here  $N_s$  denotes the number of lattice sites), systems are in the MI states. Otherwise, systems belong to either the PSF or the 2SF phases. As mentioned before, the last two phases can be distinguished by the expectation values of the atomic and the pair condensate density  $n_0 = |\langle a \rangle|^2$  and  $n_0^{\text{PSF}} = |\langle ab \rangle|^2$ , respectively. Here  $\langle a \rangle = (1/N_s) \sum_i \langle a_i \rangle$  and  $\langle ab \rangle = (1/N_s) \sum_i \langle a_i b_i \rangle$ . In the 2SF phase, one has  $n_0 \neq 0$ , while in the PSF phase one has  $n_0 = 0$  and  $n_0^{\text{PSF}} \neq 0$ .

These quantities are calculated under the combined iTEBD and TRG algorithm [20], where the ground-state wave function is assumed in the form of the tensor product state (TPS) or the projected entangled-pair state (PEPS) [27]. Due to the similarity between the present systems and the spin-1/2 bilayer spin models, the same construction of TPS as that discussed previously in Ref. [24] for the study of the bilayer systems is exploited here. Details can be found in Refs. [23, 24]. We note that the approximation in TPS can be systematically improved simply by increasing the bond dimension  $D$  of the underlying tensors. The accuracy in evaluating the expectation values for a TPS/PEPS ground state of very large systems can be systematically improved by increasing the TRG cutoff  $D_{\text{cut}}$ . In this study, we consider the bond dimension up to  $D = 5$  and keep  $D_{\text{cut}} \geq D^2$  to ensure the accuracy of the TRG calculation. As shown in the insets of the upper panels of Figs. 2 and 3, the results for  $D = 4$  seem to converge to those for larger  $D = 5$ . In the following, we take  $D = 4$  and  $D_{\text{cut}} = 25$  for systems with size  $N_s = 2^7 \times 2^7$  unless mentioned otherwise.

The results of the local order parameters defined above as functions of hopping parameter  $t$  for chemical potentials  $\mu = -0.5$  and  $-0.57$  are shown in Fig. 2. It is found that, at half filling ( $n = 1/2$ ) with  $\mu = -0.5$ , there exists a second-order quantum phase transition at  $t = t_{c,\text{PSF-2SF}} \simeq 0.081$  between the PSF and the 2SF phases. We note that, at half-filling, the particle-hole transformation for a single species (say,  $b_i \rightarrow b_i^\dagger$ ) changes the sign of interspecies interaction in Eq. (1),  $U_{ab} \rightarrow -U_{ab}$ . Therefore, at this particular filling, the results obtained for the attractive  $U_{ab}$  model can be reinterpreted in the context of the repulsive  $U_{ab}$  model and vice versa. In particular, the PSF order parameter  $\langle ab \rangle$  is mapped onto the super-counterflow (SCF) order parameter  $\langle ab^\dagger \rangle$ . Therefore, the critical value of  $t$  for the PSF-2SF transition of the attractive hard-core boson model should be the same as the SCF-2SF transition of the repulsive hard-core boson model studied previously [4, 7]. We find that our critical value of  $t$  is consistent with the result ( $t_{c,\text{PSF-2SF}} \simeq 0.092$ ) obtained by QMC method [7]. This indicates that the bond dimension used here is large enough to provide accurate findings for the present model. As shown in Fig. 2(a), within

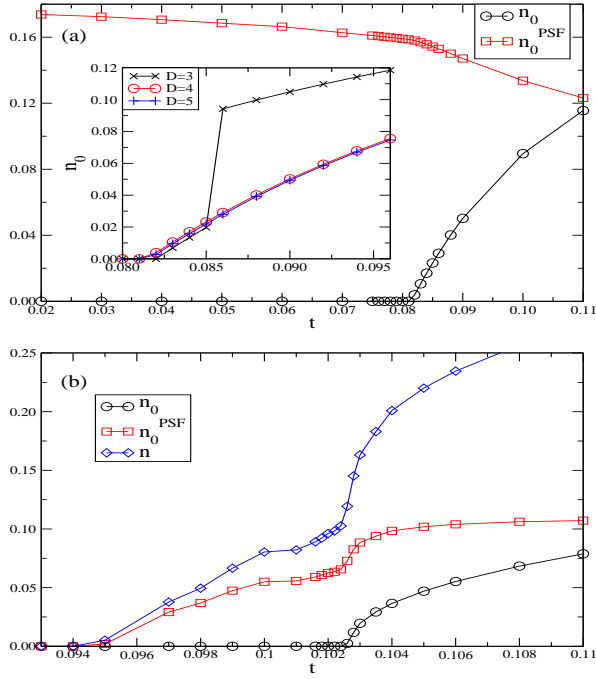


FIG. 2: (Color online) Values of particle density  $n$ , atomic condensate density  $n_0$ , and pair condensate density  $n_0^{\text{PSF}}$  for the ground states at (a)  $\mu = -0.5$  and (b)  $-0.57$  as functions of hopping parameter  $t$ . The inset in (a) illustrates the  $D$  dependence of  $n_0$ , where we use  $D_{\text{cut}} = 16$  for  $D = 3$  and  $D_{\text{cut}} = 25$  for  $D = 4, 5$ .

the PSF phase, the values of the pair condensate density  $n_0^{\text{PSF}}$  do not remain the same and are somewhat smaller than the constant value  $n_0^{\text{PSF}} = 1/4$  predicted by the mean-field theory [4]. This reduction should result from quantum fluctuations therein.

While the PSF-2SF transition at  $\mu = -0.5$  is of second order, based on the mean-field analysis, it was suggested that this transition could become first-order around the end point of the PSF-2SF phase boundary [10]. If this conclusion is true, the behavior of the first-order transition should become more apparent as the end point is approached. In Fig. 2(b),  $n$ ,  $n_0$ , and  $n_0^{\text{PSF}}$  as function of  $t$  for  $\mu = -0.57$  are displayed. A transition at  $t_{c,\text{PSF-2SF}} \simeq 0.1024$  is found, beyond which  $n_0$  becomes nonzero. Besides, anomalies in  $n$  and  $n_0^{\text{PSF}}$  occur at this transition point. Although this transition point is quite close to the end point of the PSF-2SF phase boundary as indicated in Fig. 1, we find that the transition is of second order. The same conclusions about the order of transition are reached for larger  $\mu$ 's. Nevertheless, we do observe that the order-parameter curves become more and more first-order-like as  $\mu$  decreases from  $\mu = -0.5$  to  $\mu = -0.57$  (not shown here). Our observation is consistent with the results achieved by the Monte Carlo simulation on the related classical model in Ref. [10], where only the second-order PSF-2SF transitions are found. However, one cannot completely rule out the possibility of *weakly first-order* transitions with tiny jumps in order

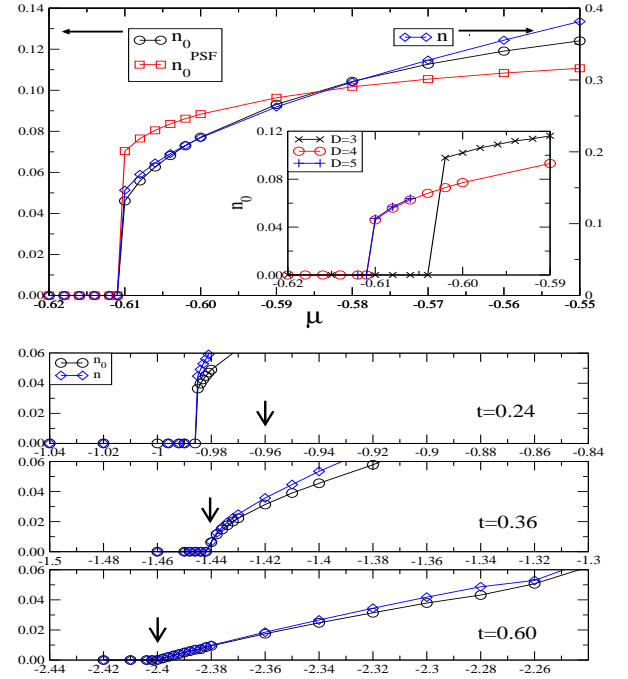


FIG. 3: (Color online) Upper panel: values of  $n$ ,  $n_0$  and  $n_0^{\text{PSF}}$  for the ground states at  $t = 0.12$  as functions of chemical potential  $\mu$ . The inset shows the  $D$  dependence of  $n_0$ , where we use  $D_{\text{cut}} = 16$  for  $D = 3$  and  $D_{\text{cut}} = 25$  for  $D = 4, 5$ . Lower panel:  $n$  and  $n_0$  as function of  $\mu$  at different  $t$ 's. The arrows denote the analytic predictions of the transition points, assuming that they are continuous transitions.

parameters when the transition points get much closer to the end point of the PSF-2SF phase boundary.

As seen in Fig. 2(b), when  $\mu = -0.57$ , an additional second-order phase transition between the  $n = 0$  MI and the PSF states appears at  $t_{c,\text{MI-PSF}} \simeq 0.094$ . In this case, the insulating state is expected to be unstable when the energy gap of pair excitation closes as  $t$  increases. Above the transition point, the lowest pair excitation starts to condense and a PSF state develops. By using the expression of the *two*-particle excitation energies relative to the  $n = 0$  state up to the third-order perturbation expansion in  $t$  [16, 28], the critical hopping parameter for this transition is found to be  $t_{c,\text{MI-PSF}} = \sqrt{(-2\mu - 1)/4z}$ , where  $z = 4$  is the coordination number for square lattices. As shown in Fig. 2(b) and Fig. 1 for cases of other  $\mu$ 's, our findings of  $t_{c,\text{MI-PSF}}$  agree well with the values given by the analytical expression. This further substantiate that the employed method can provide reliable results for the present system.

When the single-particle hopping parameter  $t$  is sufficiently large, instead of the MI-PSF transition, a direct transition from the  $n = 0$  MI state to the 2SF state as chemical potential  $\mu$  being increased becomes possible. If this MI-2SF transition is of second order, it should be induced by closing the energy gap of *single*-particle excitation. By using the analytical expression of

the one-particle excitation energies relative to the  $n = 0$  state [16, 28], the critical value of  $\mu$  at fixed  $t$  is given by  $\mu_{c, \text{MI-2SF}} = -zt$ . However, as discussed in Ref. [10], the continuous MI-2SF transitions can be preempted by the first-order ones when mutual interaction of the dilute gapped quasiparticle excitations in the MI phase is *attractive*. Due to the energy gain from the mutual attraction among quasiparticles, this first-order transition can happen before closing one-particle excitation gap. That is, the transition points for the first-order transitions would be lower than those derived by the gap closing condition. These discussions are confirmed by our calculations. In Fig. 3, our results of the local order parameters  $n$ ,  $n_0$  and  $n_0^{\text{PSF}}$  as functions of  $\mu$  for various  $t$  are plotted. For  $t = 0.12$  (upper panel), a first-order MI-2SF transition at  $\mu_{c, \text{MI-2SF}} \simeq -0.611$  is clearly observed. Upon increasing  $t$ , the jumps in the order parameters become smaller and smaller, and the transition eventually turns to be of second order (see the lower panel). For example, the MI-2SF transition at  $t = 0.6$  is found to be continuous, and it occurs at  $\mu_{c, \text{MI-2SF}} \simeq -2.4$  in agreement with the analytic formula. As shown in Fig. 3, the transition points for those first-order transitions are

always below the values given by the gap closing condition. Thus the phenomena of the transitions preempted by first-order ones is indeed demonstrated in the present systems.

To conclude, various quantum phase transitions of the two-species hard-core boson model with attractive interspecies interaction are explored under the combined iTEBD and TRG algorithm [20]. Clear evidence of a PSF phase over a finite regime in the phase diagram is provided. Critical values of system parameters at corresponding first- or second-order phase transitions are evaluated. Besides providing quantitative predictions of the phase boundaries of the proposed PSF phase, the present work also illustrates clearly the general validity and flexibility in applying the current formalism to determine quantum phase transitions in two dimensions.

We are grateful to K.-K. Ng and B. Capogrosso-Sansone for many enlightening discussions. P. Chen and M.-F. Yang thank the support from the NSC of Taiwan under Contract No. NSC NSC 98-2112-M-007-010-MY3 and NSC 96-2112-M-029-004-MY3, respectively. This work is supported also by NCTS of Taiwan.

- 
- [1] M. Lewenstein, A. Sanpera, V. Ahufinger, B. Damski, A. Sen, and U. Sen, *Adv. Phys.* **56**, 243 (2007); I. Bloch, J. Dalibard, and W. Zwerger, *Rev. Mod. Phys.* **80**, 885 (2008).
  - [2] M. Greiner, O. Mandel, T. Esslinger, T. W. Hänsch, and I. Bloch, *Nature (London)* **415**, 39 (2002).
  - [3] A. B. Kuklov and B. V. Svistunov, *Phys. Rev. Lett.* **90**, 100401 (2003).
  - [4] E. Altman, W. Hofstetter, E. Demler, and M. D. Lukin, *New J. Phys.* **5**, 113 (2003).
  - [5] A. Isacsson, M.-C. Cha, K. Sengupta, and S. M. Girvin, *Phys. Rev. B* **72**, 184507 (2005).
  - [6] S. Powell, *Phys. Rev. A* **79**, 053614 (2009).
  - [7] S. G. Şöyler, B. Capogrosso-Sansone, N. V. Prokof'ev, and B. V. Svistunov, *New J. Phys.* **11**, 073036 (2009).
  - [8] A. Hubener, M. Snoek, and W. Hofstetter, *Phys. Rev. B* **80**, 245109, (2009).
  - [9] A. Kuklov, N. Prokof'ev, and B. Svistunov, *Phys. Rev. Lett.* **92**, 030403 (2004).
  - [10] A. Kuklov, N. Prokof'ev, and B. Svistunov, *Phys. Rev. Lett.* **92**, 050402 (2004).
  - [11] S. Guertler, M. Troyer, and F.-C. Zhang, *Phys. Rev. B* **77**, 184505 (2008).
  - [12] A. Argüelles and L. Santos, *Phys. Rev. A* **75**, 053613 (2007); *ibid.* **77**, 059904(E) (2008).
  - [13] L. Mathey, I. Danshita, and C. W. Clark, *Phys. Rev. A* **79**, 011602(R), (2009).
  - [14] A. Hu, L. Mathey, I. Danshita, E. Tiesinga, C. J. Williams, and C. W. Clark, *Phys. Rev. A* **80**, 023619 (2009).
  - [15] C. Menotti and S. Stringari, *Phys. Rev. A* **81**, 045604 (2010).
  - [16] M. Iskin, arXiv:1001.0021v2.
  - [17] C. Trefzger, C. Menotti, and M. Lewenstein, *Phys. Rev. Lett.* **103**, 035304 (2009).
  - [18] E. L. Pollock and D. M. Ceperley, *Phys. Rev. B* **36**, 8343 (1987).
  - [19] L. Pollet, M. Troyer, K. Van Houcke, and S. M. A. Rombouts, *Phys. Rev. Lett.* **96**, 190402 (2006); L. Pollet, Ph.D. thesis, Universiteit Gent, 2005 (unpublished).
  - [20] H. C. Jiang, Z. Y. Weng, and T. Xiang, *Phys. Rev. Lett.* **101**, 090603 (2008); Z. Y. Xie, H. C. Jiang, Q. N. Chen, Z. Y. Weng, and T. Xiang, *ibid.* **103**, 160601 (2009).
  - [21] G. Vidal, *Phys. Rev. Lett.* **98**, 070201 (2007); R. Orús and G. Vidal, *Phys. Rev. B* **78**, 155117 (2008).
  - [22] M. Levin and C. P. Nave, *Phys. Rev. Lett.* **99**, 120601 (2007); Z. C. Gu, M. Levin, and X. G. Wen, *Phys. Rev. B* **78**, 205116 (2008).
  - [23] P. Chen, C.-Y. Lai, and M.-F. Yang, *J. Stat. Mech.: Theory Exp.* (2009), P10001.
  - [24] P. Chen, C.-Y. Lai, and M.-F. Yang, *Phys. Rev. B* **81**, 020409 (2010).
  - [25] H. H. Zhao, Z. Y. Xie, Q. N. Chen, Z. C. Wei, J. W. Cai, and T. Xiang, *Phys. Rev. B* **81**, 174411 (2010).
  - [26] W. Li, S.-S. Gong, Y. Zhao, and G. Su, *Phys. Rev. B* **81**, 184427 (2010).
  - [27] T. Nishino *et al.*, *J. Phys. Soc. Jpn* **67**, 3066, (1998); Y. Nishio *et al.*, arXiv:cond-mat/0401115; J. Jordan *et al.*, *Phys. Rev. Lett.* **101**, 250602 (2008); J. Jordan *et al.*, *Phys. Rev. B* **79**, 174515 (2009); R. Orús and G. Vidal, *ibid.* **80**, 094403 (2009). For a recent review, see J. I. Cirac and F. Verstraete, *J. Phys. A* **42**, 504004 (2009).
  - [28] By setting  $t_{\uparrow} = t_{\downarrow} = t$ ,  $U_{\uparrow\downarrow} = U_{ab}$ ,  $\mu_{\uparrow} = \mu_{\downarrow} = \mu$ , and  $n_{\uparrow} = n_{\downarrow} = n = 0$ , the one-particle and the two-particle excitation gaps can be obtained from Eqs. (8) and (11) of Ref. [16], respectively.